STOCHASTIC INSULIN SENSITIVITY MODELS FOR TIGHT GLYCAEMIC CONTROL

J. Geoffrey Chase*, Jessica Lin*, Dominic S Lee, Jason Wong*, Christopher E. Hann* and Geoffrey M. Shaw*****

**Centre for Bioengineering, University of Canterbury, Christchurch, New Zealand*
**Dept of Mathematics & Statistics, University of Canterbury, New Zealand*
****Department of Intensive Care Medicine, Christchurch Hospital, Christchurch, New Zealand*

Abstract: Hyperglycaemia is prevalent in critical care, and tight control reduces mortality. Targeted glycaemic control can be achieved by frequent fitting and prediction of a modelled insulin sensitivity index, S_I. However, this parameter varies significantly in the critically ill as their condition evolves. A 3-D stochastic model of hourly S_I variability is constructed using retrospective data from 18 critical care patients. The model provides a blood glucose level probability distribution one hour following an intervention, enabling accurate prediction and more optimal glycaemic control.

Keywords: Biomedical Control, Non-Linear Models, Physiological Models, Physiology, Stochastic Modelling, Markov Models, Medical Systems.

1. INTRODUCTION

Hyperglycaemia and severe insulin resistance are prevalent in the critically ill, and tight control can reduce mortality up to 45% (Van den Berghe et al., 2001). Chase et al. (2005a) clinically verified a targeted control algorithm that accounts for inter-patient variability and evolving physiological condition. The adaptive control approach identifies patient dynamics, particularly insulin sensitivity, to determine the best control input. Hence better understanding and modelling of patient variability in the ICU can lead to better glycaemic management.

Therefore, the ultimate goal of this study is to produce model-base blood glucose confidence bands to optimise glycaemic control. These bands are based on stochastic models developed from clinically observed model-based variations, and allow targeted control with user specified confidence on the glycaemic outcome.

2. METHODS

2.1 Glucose-Insulin System Model

This study uses a patient-specific glucose-insulin system model from Chase et al. (2005a). It accounts for time-varying insulin sensitivity and endogenous glucose removal, and two saturation kinetics.

$$\dot{G} = -p_G G - S_I (G + G_E)\frac{Q}{1+\alpha_G Q} + P(t) \quad (1)$$

$$\dot{Q} = -kQ + kI \quad (2)$$

$$\dot{I} = -n\frac{I}{1+\alpha_I I} + \frac{u_{ex}(t)}{V_I} \quad (3)$$

where G and I denote the glucose above an equilibrium level, G_E, and the plasma insulin from an exogenous insulin input. Insulin utilization over time is Q, with effective insulin decay rate k. Endogenous glucose removal and insulin sensitivity are p_G and S_I. Insulin distribution volume is V_I, and n is plasma insulin decay. External nutrition and insulin input are $P(t)$ and $u_{ex}(t)$. Michaelis-Menten saturation in plasma insulin disappearance and insulin-stimulated glucose removal are defined by α_I and α_G.

Insulin sensitivity, S_I, is the critical parameter that drives the dynamic system response to exogenous insulin. This value changes with the severity of illness, and thus captures the evolution of the patient's insulin resistance and condition. Hence, identifying S_I over time is critical to providing safe, tight glycaemic control. It will also enable better prediction of the outcome of an intervention. However, no such models or data currently exist.

2.2 Stochastic Model

Patient-specific parameters, p_G and S_I, are fitted to long term retrospective clinical data from 18 patients from a 201-patients data audit (Shaw et al., 2004). Parameter identification is performed with an integration-based method developed by Hann et al. (2005). Each patient record spans at least one day with data every three-hours or less. This cohort broadly represents the cross section of patients seen in the ICU, regarding medical condition, age, sex, APACHE II scores and mortality.

Zero order piecewise linear functions are used to define p_G and S_I, with a discontinuity every two hours for p_G and every hour for S_I because greater variability in S_I is previously identified (Hann et al., 2005). Table 1 shows the parameter values (Chase et al., 2005a).

Table 1: Generic parameter values

Parameter	Unit	Value
α_G	*L/mU*	1/65
α_I	*L/mU*	0.0017
n	min^{-1}	0.16
k	min^{-1}	0.0198
V_I	*L*	3.15

The fitted p_G and S_I data reveals that the variability of both parameters is dependent on its present value. The distribution of fitted S_I is shown by the dots in Figure 1. The probability distribution of potential S_I, shown by the probability bands, clearly varies with its value across the horizontal axis.

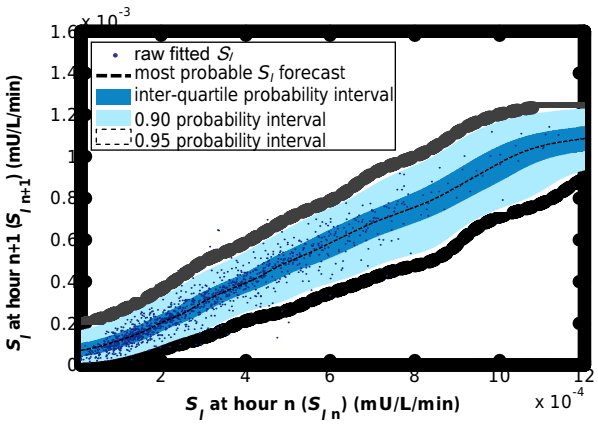

Figure 1: Fitted S_I and probability intervals

Thus, the variations in S_I can be treated as a Markov process. A Markov process has the property that the conditional probability distribution of future states of the process, given the present state, depends only upon the current state. Therefore, using the Markov property of the stochastic behaviour of S_I, the conditional probability distribution of $S_{I\,n+1}$ taking on a value y can be calculated by knowing $S_{I\,n} = x$:

$$P(S_{I\,n+1} = y \mid S_{I\,n} = x) = \frac{P(S_{I\,n} = x, S_{I\,n+1} = y)}{P(S_{I\,n} = x)} \quad (4)$$

Considering the fitted S_I in a 2-D space, as shown in Figure 1, the joint probability function across the x-y ($S_{I\,n}$ - $S_{I\,n+1}$) plane is defined by the fitted values shown by the dots whose coordinates are x_i and y_i,

$$P(x, y) = \frac{1}{n}\sum_{i=1}^{n} \frac{\phi(x; x_i, \sigma_{x_i}^{\,2})}{p_{x_i}} \frac{\phi(y; y_i, \sigma_{y_i}^{\,2})}{p_{y_i}} \quad (5)$$

$$p_{x_i} = \int_0^{\infty} \phi(x; x_i, \sigma_{x_i}^{\,2}) \quad (6)$$

$$p_{y_i} = \int_0^{\infty} \phi(y; y_i, \sigma_{y_i}^{\,2}) \quad (7)$$

Effectively, the 2-D joint probability function is the normalised summation of normal probability distribution functions $\phi(x; x_i, \sigma_{x_i}^{\,2})$ centred at individual data points.

To illustrate a 3-D map in the mind, consider this numerical operation as a sand building exercise. If the first quadrant of the x-y ($S_{I\,n}$ - $S_{I\,n+1}$) plane, as shown in Figure 1, is where the sand box is confined in, and that a pile of sand of a cubic unit is dropped onto every dot in Figure 1, then the resulted sand sculpture is the simple representation of the joint probability $P(x, y)$ on the x-y ($S_{I\,n}$ - $S_{I\,n+1}$) plane. In Equations (5)-(7), the variance σ at each data point is a function of the local data density in a centred and orthonormalised space of x and y. Putting Equations (6) and (7) into Equation (5) normalises each $\phi(x; x_i, \sigma_{x_i}^{\,2})$ and $\phi(y; y_i, \sigma_{y_i}^{\,2})$ in the positive domain. This, in the sand building exercise example, effectively puts boundaries along $x = 0$ and $y = 0$, confining sand to stay in the first quadrant, and therefore forces physiological validity in S_I values.

In Equation (4), the right hand side denominator can be calculated by integrating Equation (5) with respect to y. Hence, Equation (5) can be calculated:

$$P(S_{I\,n+1} = y \mid S_{I\,n} = x) = \sum_{i=1}^{n} \omega_i(x) \frac{\phi(y; y_i, \sigma_{y_i}^{\,2})}{p_{y_i}} \quad (8)$$

$$\omega_i(x) = \frac{\phi(x; x_i, \sigma_{x_i}^{\,2}) / p_{x_i}}{\sum_{j=1}^{n} \phi(x; x_j, \sigma_{x_j}^{\,2}) / p_{x_i}} \quad (9)$$